Molybdenum Sequestration in *Brassica* Species. A Role for Anthocyanins?[1]

Kerry L. Hale, Steve P. McGrath, Enzo Lombi, Stephen M. Stack, Norman Terry, Ingrid J. Pickering, Graham N. George, and Elizabeth A.H. Pilon-Smits*

Department of Biology, Anatomy/Zoology Building, Colorado State University, Fort Collins, Colorado 80523 (K.L.H., S.M.S., E.A.H.P.-S.); Agriculture and Environment Division, Institute of Arable Crops Research-Rothamsted, Harpenden, Hertfordshire AL5 2JQ, United Kingdom (S.P.M., E.L.); Department of Plant and Microbial Biology, 111 Koshland Hall, University of California, Berkeley, California 94270 (N.T.); and Stanford Synchrotron Research Laboratory (SSRL), Stanford Linear Accelerator Center, P.O. Box 20450, Stanford, California 94309 (I.J.P., G.N.G.)

To elucidate plant mechanisms involved in molybdenum (Mo) sequestration and tolerance, *Brassica* spp. seedlings were supplied with molybdate, and the effects on plant physiology, morphology, and biochemistry were analyzed. When supplied with (colorless) molybdate Indian mustard (*Brassica juncea*) seedlings accumulated water-soluble blue crystals in their peripheral cell layers. Energy dispersive x-ray analysis showed that Mo accumulated predominantly in the vacuoles of the epidermal cells. Therefore, the blue crystals are likely to be a Mo compound. The x-ray absorption spectrum of the plant-accumulated Mo was different than that for molybdate, indicating complexation with a plant molecule. Because the blue compound was water soluble and showed a pH-dependent color change, possible involvement of anthocyanins was investigated. An anthocyanin-less mutant of *Brassica rapa* ("fast plants") was compared with varieties containing normal or high anthocyanin levels. The anthocyanin-less mutant did not show accumulation of a blue compound when supplied with molybdate. In the anthocyanin-containing varieties, the blue compound colocalized with anthocyanins in the peripheral cell layers. Mo accumulation by the three *B. rapa* varieties was positively correlated with anthocyanin content. Addition of molybdate to purified *B. rapa* anthocyanin resulted in an in vitro color change from pink to blue. Therefore, Mo appears to be sequestered in vacuoles of the peripheral cell layers of *Brassica* spp. as a blue compound, probably a Mo-anthocyanin complex.

Molybdenum (Mo) is an essential micronutrient for plants, bacteria, and animals. Mo-deficient plants exhibit poor growth and low chlorophyll and ascorbic acid content (Marschner, 1995). Mo is also a component of some bacterial nitrogenases, and therefore is especially important for plants that live in symbiosis with nitrogen-fixing bacteria. The major metabolic function for Mo in eukaryotic organisms is as an essential component of the mononuclear Mo enzymes (Hille, 1996), which play roles in many key metabolic processes such as sulfur detoxification, purine catabolism, nitrate assimilation, and phytohormone synthesis in plants (Stallmeyer et al., 1999). These enzymes usually (but not always) catalyze two-electron redox reactions that are coupled to the transfer of an oxygen atom to or from substrate and the metal, during which the Mo cycles between the Mo(VI) and Mo(IV) oxidation states. In these systems, Mo is bound to the dithiolene of a novel pyranopterin cofactor that is known as molybdopterin (Hille, 1996). Although a low-M_r species containing both Mo and molybdopterin has never been properly characterized, this complex is known as the Mo cofactor (Moco). These enzymes are unrelated to the Mo-containing nitrogenase of nitrogen-fixing bacteria that contain a Mo-iron-sulfur cluster.

A mutational block in the early steps of Moco biosynthesis leads to the combined loss of function of Mo enzymes. As a result, plant cells can no longer assimilate inorganic nitrogen and have altered levels of certain phytohormones (Seo et al., 1998). However, a change in proteins catalyzing the last step of Moco synthesis, i.e. the transfer and incorporation of Mo into molybdopterin, leads to a molybdate repairable phenotype (Falciani et al., 1994), whereby the addition of molybdate is sufficient to overcome the negative effects of the mutation. Therefore, molybdate is thought to be the source of Mo for incorporation into Moco (Kuper et al., 2000).

[1] This work was supported by the National Science Foundation (Career Development Grant no. 9982432) and by the Environmental Protection Agency (Research Grant no. G8A11586 to E.A.H.P.-S.). The XAS experiments were made possible through SSRL Synchrotron beam time (granted to N.T.). SSRL is funded by the U.S. Department of Energy, Offices of Basic Energy Sciences and Biological and Environmental Research; by the National Institutes of Health; by the National Center for Research Resources, by the Biomedical Technology Program; and by the National Institute of General Medical Sciences. The Institute of Arable Crops Research-Rothamsted receives grant-aided support from the Biotechnology and Biological Sciences Research Council of the UK.

* Corresponding author; e-mail: epsmits@lamar.colostate.edu; fax 970–491–0649.

In plants, Mo is readily mobile in xylem and phloem for long-distance transport (Kannan and Ramani, 1978), though little is known of the mechanisms involved in Mo homeostasis. Molybdate competes with sulfate for uptake at the root surface, suggesting a common uptake mechanism (Stout et al., 1951). However, it has also been suggested that molybdate is taken up by a phosphate transporter (Heuwinkel et al., 1992). Furthermore, a recent study by Palmgren and Harper (1999) suggests the presence of a Mo-specific metal transporter, AMA1, in Arabidopsis. T-DNA knockout mutants, where AMA1 was rendered ineffective, showed 5-fold reduced Mo accumulation, but no reduction in any other essential micronutrients.

The Mo content of plants is a direct reflection of the bioavailability of Mo in the soil. The relation of Mo influx versus concentration is approximately linear in soil systems (Barber, 1995). Bioavailability of Mo is positively correlated with soil pH (Karmian and Cox, 1978). In acidic soils, Mo deficiency in plants is common. On the other hand, in some soils of high pH, plants may accumulate enough Mo for ruminants feeding on the plants to develop molybdenosis. Molybdenosis is caused by an imbalance of Mo and copper in the ruminant diet, which induces a copper deficiency (Stark and Redente, 1990). Plants supplied with adequate Mo usually contain 1 to 2 mg kg^{-1} Mo; plant material containing an excess of 5 mg kg^{-1} Mo is sufficient to cause molybdenosis in ruminant animals (Barber, 1995). Molybdenosis in livestock occurs in the western U.S., often in soils with poor drainage and high organic matter (Gupta and Lipsett, 1981). Mo pollution due to mining and stainless steel industry poses a serious environmental problem at several locations in the U.S., including several Superfund sites (polluted sites in the U.S. designated by the U.S. Environmental Protection Agency for high priority remediation). Plant samples from a mining site near Empire, CO were found to contain up to 400 mg kg^{-1} Mo (Trlica and Brown, 2000). Phytoremediation, the use of plants to remediate environmental pollution, may prove to be a viable strategy for remediating Mo in these areas, either via phytoextraction (accumulation in harvestable plant parts) or phytostabilization (in situ immobilization).

To use plants optimally for Mo remediation, we need to know which processes are involved and where rate limitations may occur. The goal of this study was to obtain a better understanding of plant mechanisms that control accumulation, tolerance, and biotransformation of Mo in plants.

RESULTS

When Indian mustard (*Brassica juncea*) seedlings were grown on agar medium containing different concentrations of colorless ammonium molybdate, they showed blue coloration, especially at the base of the hypocotyl and around the petioles (Fig. 1, A–C). Cross sections of the Mo-treated seedlings showed that the blue compound was present in a crystal-like form (Fig. 1, C and D), localized predominantly in the epidermal and subepidermal tissues (Fig. 1E). Seedlings grown without Mo did not show this blue coloration (Fig. 1F). A similar distribution was observed when mature plants were supplied with ammonium molybdate, with the blue coloration being most pronounced in the stem and near vascular tissue in the leaves (results not shown).

To determine whether the blue compound contained Mo, we used two approaches. First, we compared the Mo concentrations in tissues of bluer seedlings with those of seedlings that had less blue coloration from the same treatment (Fig. 2). Stem and leaf samples from bluer seedlings contained significantly higher Mo concentrations than did those for less blue seedlings. In the second approach, energy dispersive x-ray analysis (EDXA) was used to determine the localization of Mo. Mo was accumulated primarily in the epidermal cells of the hypocotyl (Fig. 3), correlating with the location of the blue compound. Dot maps of EDXA analyses show that the concentration of Mo was low in the cell walls, whereas most Mo was located in the vacuoles. No association with K or P was observed (Fig. 3). The concentration of Mo in the vacuoles of epidermal cells was calculated to be 33.7 ± 5.4 mM (SE; $n = 23$). Larger cells (30–50 μm) contained significantly higher Mo concentrations (49.6 ± 6.1 mM) than smaller (approximately 10 μm) cells (13.1 ± 2.4 mM). The concentration of Mo in the mesophyll was below the EDXA detection limit for Mo (<10 mM). Thus, results from this approach again indicate that the blue color results from the presence of Mo.

X-ray absorption spectroscopy (XAS) was used to provide details of the chemical form of Mo present in the plant tissues. Molybdate in aqueous solution exists as the $[MoO_4]^{2-}$ anion in basic conditions, but at acidic pH levels (i.e. below about pH 6) the $[MoO_4]^{2-}$ anion protonates to form water and polymolybdate anions, the simplest of which is paramolybdate $[Mo_7O_{24}]^{6-}$, which is formed of seven edge-sharing octahedra. The coordination geometry of Mo thus changes from pure tetrahedral high pH, to octahedral at low pH, and the mean number of oxo groups per Mo is reduced from four to two for $[Mo_7O_{24}]^{6-}$, or to even smaller values for the higher polymolybdate anions. As shown in Figure 4A, the Mo K near-edge spectrum from the plant differs from that of aqueous $[MoO_4]^{2-}$ and $[Mo_7O_{24}]^{6-}$ standards, with some resemblance to the polymolybdate. In particular, the pronounced pre-edge peak observed in both molybdate spectra is somewhat lower in intensity in the shoot spectrum. This peak can be assigned to a 1 s → 4 d transition, which is dipole forbidden with a small quadrupole-allowed intensity, although in noncentrosymmetric environments mixing of 5 p with 4

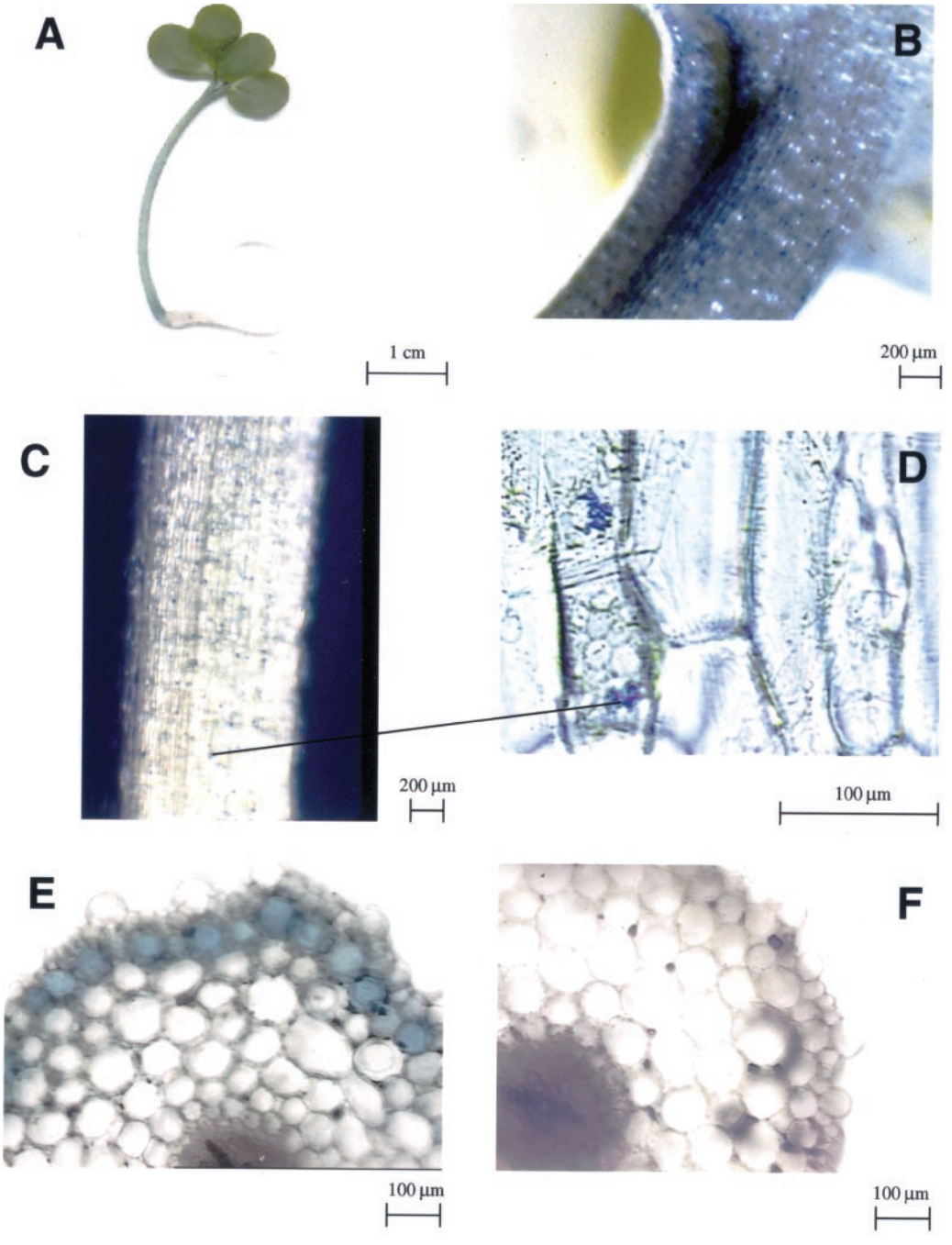

Figure 1. Indian mustard seedlings grown for 7 d in agar medium, with (A–E) or without (F) 60 mg L^{-1} ammonium molybdate. A, Seedling. B, Close-up of petiole. C, Close-up of hypocotyl. D, Longitudinal section of hypocotyl at higher magnification to show irregular blue precipitate in some epidermal cells. The black line connects the precipitate at low and high magnification. E, Cross section of hypocotyls showing blue color in the peripheral cell layers. F, Hypocotyl cross section of a seedling grown without Mo.

d levels confers significant dipole-allowed intensity (Kutzler et al., 1980). The intensity of this feature has been observed to correlate with the number of Mo = O (oxo) ligands to Mo, which is consistent with the smaller intensity observed for $[Mo_7O_{24}]^{6-}$ versus $[MoO_4]^{2-}$. In the plant spectrum, its reduced presence suggests a smaller number of oxo groups (e.g. around two).

The EXAFS spectrum (Fig. 4B) of Mo in plant shoots confirms that the Mo is modified from the simple $[MoO_4]^{2-}$ structure, which consists of four Mo = O interactions at 1.76 Å. The shoot spectrum indicates several different interactions in the first shell, and there is also evidence for longer range interactions at >3 Å. Curve fitting of the data (Table I) indicates three different Mo − O distances in the

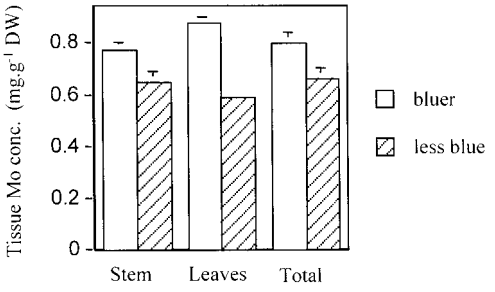

Figure 2. Tissue Mo concentration in Indian mustard seedlings grown for 7 d on agar medium containing 60 mg L^{-1} ammonium molybdate. Stem or leaf tissue collected from bluer seedlings contained higher Mo concentrations ($P < 0.05$, $n = 3$) than comparable organs of less blue seedlings. Values represent the mean ± SE of three samples pooled from 36 seedlings each.

first shell, at 1.72, 1.96, and 2.23 Å, and models the outer shells as two different Mo···Mo interactions at 3.15 and 3.35 Å. This is consistent with a polymolybdate-type cluster in the plant. $[Mo_7O_{24}]^{6-}$, for example, has Mo = O bonds at 1.71 to 1.72 Å, with Mo-O bonds cis to oxo ligands at about 1.89 to 2.00 Å and Mo-O bonds trans to Mo = O bonds at 2.1 to 2.5 Å. Considering the heterogeneity in bond lengths, this is in excellent agreement with our curve-fitting results. The Mo-Mo distances in $[Mo_7O_{24}]^{6-}$ form two obvious groups at 3.20 to 3.28 Å and 3.41 to 3.45 Å, which compares reasonably well with our analysis, especially because the EXAFS from these will include multiple scattering that was neglected in our simple analysis. Taken together, the spectroscopic evidence strongly suggests the presence of a polymolybdate species in the plant.

To further investigate the chemical nature of the blue compound produced by Indian mustard when exposed to Mo, ground plant tissue was extracted with different solvents (water, methanol, acetone, and chloroform). The blue compound was found to be most soluble in water, though it appears to precipitate at higher concentrations, forming crystal-like structures as those seen in Figure 1. Alteration of the pH with either HCl or NaOH caused the color of the aqueous extract to change from blue to either pink (pH < 3.4) or yellow (pH > 7.2). This color change was reversible (results not shown). Mo K near-edge spectra of the extracts at different pH are shown in Figure 4A. As expected from simple chemistry (see above) the spectrum of the high pH (yellow) extract resembled that of aqueous $[MoO_4]^{2-}$, whereas those of both pink and blue low-pH forms were slightly different from each other, similar to the spectrum of the shoots, and are consistent with polymolybdates.

Because pH-dependent color change is a property of anthocyanins, we wanted to test the involvement of anthocyanins in the formation of blue compounds, Mo tolerance, and Mo accumulation. To this end, we made use of different varieties of rapid-cycling *B.*

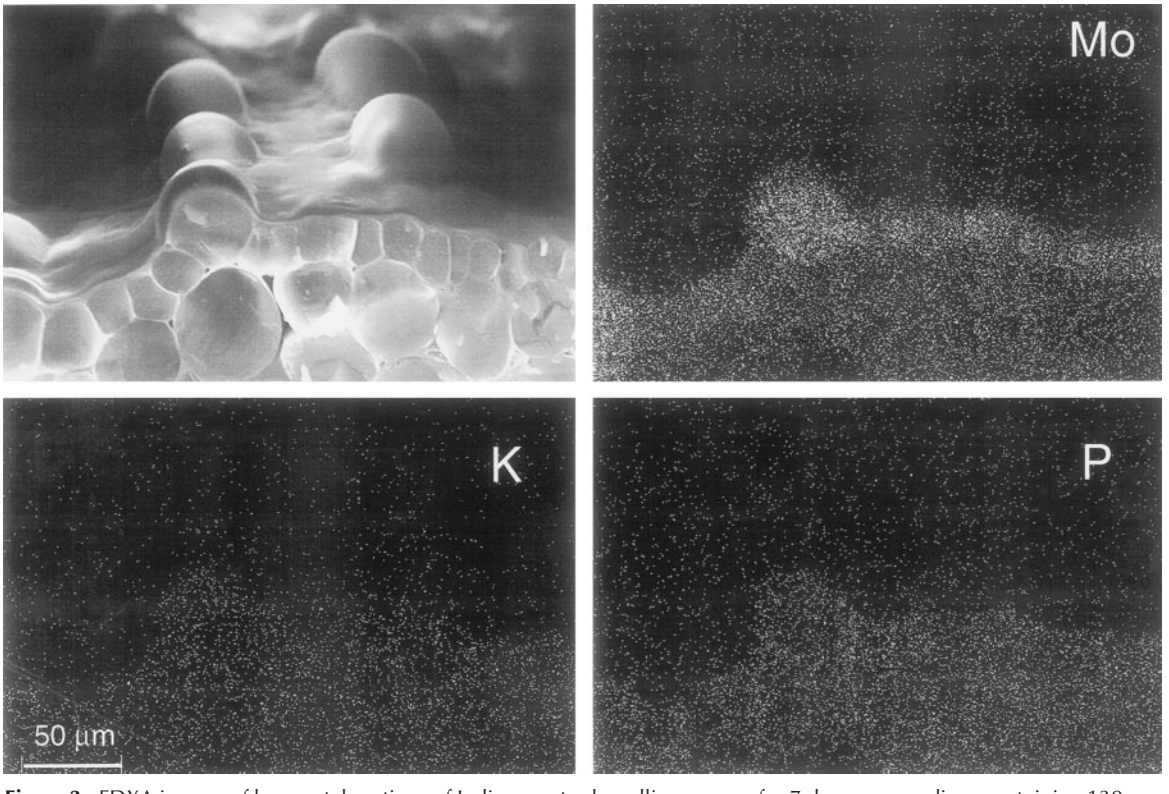

Figure 3. EDXA images of hypocotyl sections of Indian mustard seedlings grown for 7 d on agar medium containing 130 mg L^{-1} ammonium molybdate. Mo is present mainly in the epidermis (top right image), whereas K and P are evenly distributed throughout the tissue (bottom).

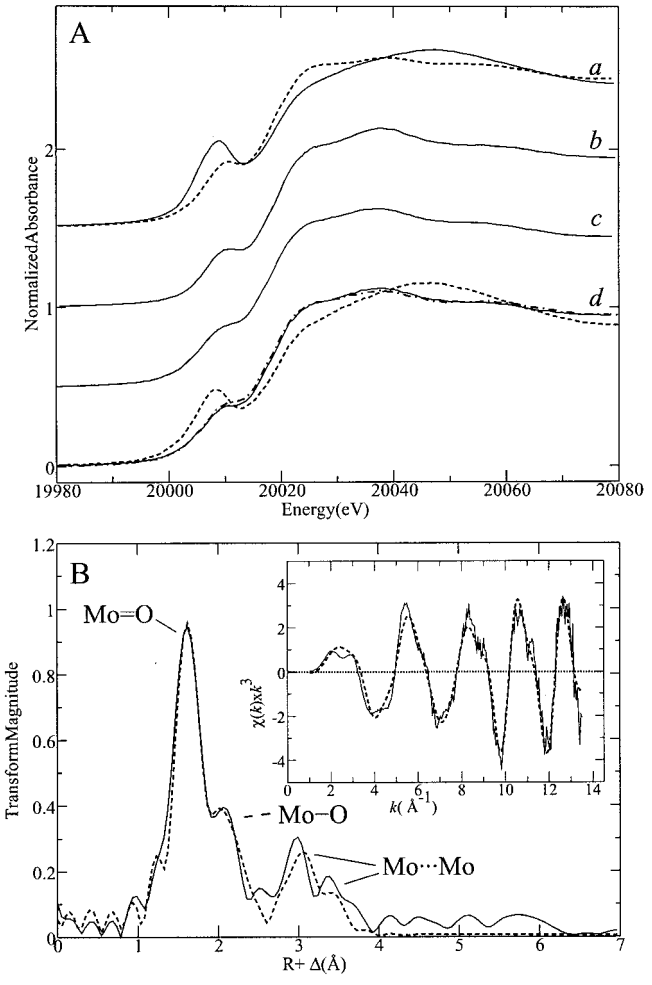

Figure 4. XAS of Mo in Indian mustard seedlings grown for 7 d on agar medium containing 60 mg L^{-1} ammonium molybdate. A, Mo K x-ray absorption near-edge spectra of: a, Molybdate in aqueous solution at pH 8 (solid line) and pH 4 (dashed line); b, Indian mustard seedlings; c, *Brassica rapa* anthocyanin-less mutant; and d, aqueous extracts of Indian mustard at pH 8 (dashed line), pH 6 (solid line), and pH 4 (dot-dashed line). B, Results of extended x-ray absorption fine structure (EXAFS) curve fitting of shoots of Indian mustard seedlings. Inset, The k^3-weighted Mo K-edge EXAFS oscillations for the experimental data (solid line) and the best fit (dashed line) according to the parameters in Table I. The main panel shows the corresponding Fourier transforms, phase corrected for the first shell Mo-O interactions.

rapa ("fast plants") that vary in anthocyanin production. A mutant unable to produce anthocyanin (C1-108) was compared with intermediate anthocyanin (C1-34) and high anthocyanin (C1-67) varieties. When grown in the presence of Mo, the anthocyanin-less mutant did not show the blue coloration, and the high anthocyanin variety was bluer than the variety containing intermediate anthocyanin levels (Fig. 5A). Thus, the degree of blueness was related to anthocyanin content. The Mo K near-edge spectrum of shoot tissue of the *B. rapa* anthocyanin-less mutant (Fig. 4A) appeared similar to that of the Indian mustard shoot tissue, but with a less pronounced pre-edge peak.

To visualize the distribution of the colored compounds, *B. rapa* varieties grown with and without Mo were cross-sectioned and the presence of blue compounds and anthocyanins were compared. anthocyanin-less mutants exposed to Mo showed no accumulation of the blue compound (Fig. 5B, left). There was no observable difference between treated and non-treated (not shown) cross sections of anthocyanin-less plants. In the anthocyanin-containing varieties, the anthocyanin was shown to be concentrated in the peripheral cell layers (Fig. 5B, middle), as was the blue compound that was produced when the plants were treated with Mo (Fig. 5B, right). Therefore, the tissue distribution of anthocyanin is similar to that of the blue compound.

To determine the possible role of anthocyanins in Mo accumulation and tolerance, we compared shoot Mo concentrations, fresh weights, and root lengths of the three *B. rapa* varieties. In a first experiment, seeds were sterilized using a standard procedure with ethanol and bleach. The results showed a distinct relationship between anthocyanin content and Mo tolerance (Table II) and accumulation (Fig. 6A). There was no difference in tolerance to the bleach treatment alone; therefore, it is unlikely that the relationships between anthocyanin and Mo tolerance or accumulation is an artifact of differential bleach tolerance. However, because germination frequencies were rather low after the bleach and ethanol treatment (especially for C1-108), a second experiment was done where seeds were sterilized using plant preservative mixture (PPM) to deter infection without the potential harm that bleach and ethanol may cause. Again, there was a significant difference in Mo accumulation between the anthocyanin-less and anthocyanin-containing varieties (Fig. 6B). However, there was no clear correlation between Mo tolerance and anthocyanin content, except for fresh weight at 60 mg L^{-1} Mo (Table III) Please note that because we were unable to grow C1-34 seedlings without infection on PPM, no data are available for that genotype.

Table I. *EXAFS curve fitting of molybdate and molybdate transformed in plant shoots*

Coordination no. was fitted to the nearest integer. The nos. in parentheses after the distances and Debye-Waller factors indicate the precisions, expressed as three times the estimated SDs (obtained from the diagonal elements of the covariance matrix) in the last digit(s) of the values. The accuracies will be larger than, and related to, the precisions, and will typically be less than ±0.02 Å for interatomic distances.

Sample	No. and Type	Distance	Debye-Waller Factor
		Å	Å²
Molybdate	4 Mo-O	1.767 (3)	0.0025 (3)
Mo-treated shoots	3 Mo-O	1.719 (5)	0.0048 (5)
	2 Mo-O	1.964 (8)	0.0041 (10)
	1 Mo-O	2.23 (2)	0.004 (2)
	1 Mo. . .Mo	3.15 (1)	0.0068 (12)
	1 Mo. . .Mo	3.35 (2)	0.0068 (12)

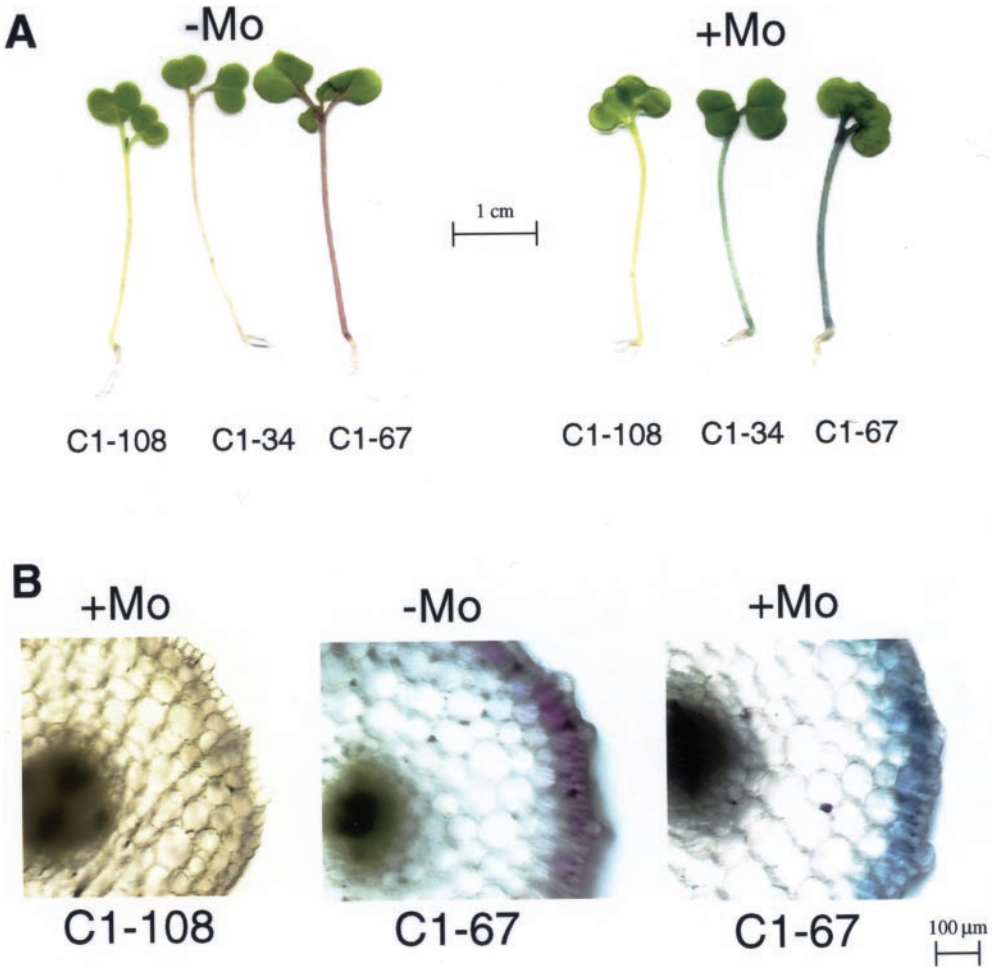

Figure 5. Mo-induced blueness is correlated with anthocyanin content. A, *B. rapa* seedlings were grown for 7 d on agar medium in the absence (left) or presence (right) of 30 mg L^{-1} ammonium molybdate. Three varieties were used, with different anthocyanin levels: anthocyanin-less (C1-108), intermediate anthocyanin content (C1-34), and high anthocyanin content (C1-67). B, Cross sections of different *B. rapa* varieties grown for 7 d on agar medium with or without 60 mg L^{-1} ammonium molybdate. Left, anthocyanin-less mutant (C1-108) grown in the presence of molybdate; middle, right, high-anthocyanin variety (C1-67) grown in the absence (middle), or the presence (right) of molybdate. Blue crystals similar to those found in Indian mustard were present in the Mo-treated *B. rapa* C1-67 seedlings, although difficult to see at this magnification.

In a last experiment, no sterilization procedure was used. Every box of seedlings used for this experiment had some microbial infection; therefore, growth data were not recorded. Individual seedlings that were not infected were removed, washed, and tested for Mo content. Once again, there was a relationship between Mo accumulation and anthocyanin content (Fig. 6C). Please note that there were no C1-34 seedlings left uninfected after 7 d; therefore, C1-34 data are not shown.

Because it is not known which step in the anthocyanin biosynthesis pathway is affected in mutant C1-108, several experiments were performed to confirm that anthocyanins are responsible for the observed effects, and not some other product of this pathway. First, seedlings of the three varieties were treated with a methanol/HCl solution overnight to extract anthocyanins (and other flavonoids). This crude extract was brought up to vacuolar pH 5 (Fig. 7A, left), and molybdate was added. The anthocyanin-less extract remained colorless even after the addition of Mo, whereas the C1-34 and C1-67 extracts immediately turned bright blue (Fig. 7A, middle). The pH of the extracts after Mo addition did not change significantly; therefore, this phenomenon is not the result

Table II. *Mo tolerance of bleach-sterilized B. rapa varieties*

Seedlings were grown for 7 d on agar medium containing 30 mg L^{-1} Mo ammonium molybdate. Values shown represent relative growth, calculated as: (growth + Mo/growth − Mo) × 100% (mean ± SE, $n = 36$). P values represent a statistical comparison with the C1-108 line. C1-108, Anthocyaninless variety; C1-34, wild type; C1-67, high anthocyanin variety.

Variety	Fresh Wt	Root Length
C1-108	35 ± 5	32 ± 11
C1-34	55 ± 4 ($P < 0.05$)	66 ± 11 ($P < 0.05$)
C1-67	63 ± 5 ($P < 0.05$)	56 ± 6 ($P < 0.05$)

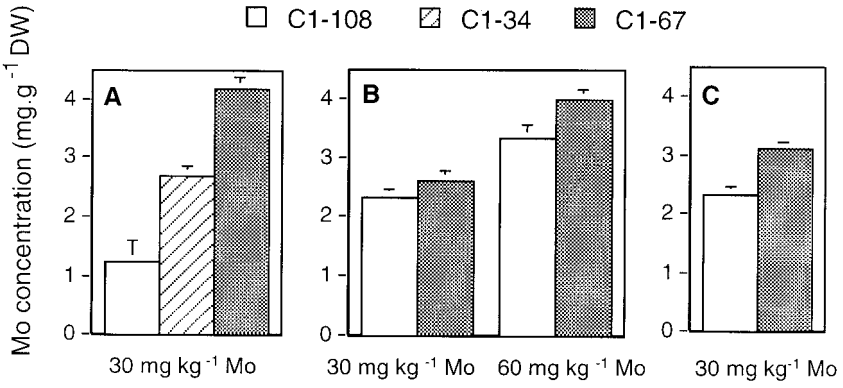

Figure 6. Shoot Mo concentrations in seedlings of different *B. rapa* varieties grown for 7 d on agar medium with ammonium molybdate. The seeds were either bleach sterilized (A), plant preservative mixture (PPM; Plant Cell Technology, Inc., Washington, DC) sterilized (B), or not sterilized (C). The Mo concentration in the anthocyanin-less mutant (C1-108) was significantly lower than in C1-34 or C1-67 in all cases ($P < 0.05$, $n = 5$) except in experiment B at 30 ppm Mo, where $P < 0.10$ ($n = 5$).

of a simple change in pH. Extract from the C1-34 variety was further purified using paper chromatography, brought up to vacuolar pH, and molybdate was added. The blue color change immediately occurred (Fig. 7A, right) giving further evidence that anthocyanins are involved in the formation of blue compounds in these *B. rapa* seedlings.

Second, to determine the presence of flavonols (direct precursors of anthocyanins) within the plant tissue of the C1-108 mutants, seedlings of each *B. rapa* variety were treated with diphenylboric-acid-2-aminoethyl ester (DPBA) to visualize the fluorescence of flavonols. In cross-sectional comparisons with C1-34 (and C1-67, not shown), the anthocyanin-less mutants appear to have greater accumulation of flavonols (Fig. 7B, left), which stain orange-yellow under a UV light source with a DAPI filter. Therefore, flavonols appear to be present in the C1-108 mutant, and, because they appear to be accumulated, the mutation may be at the dihydroflavonol reductase step (conversion of flavonols to leucoanthocyanidins). We also used paper chromatography of crude anthocyanin extracts from all three varieties, and compared autofluorescence under a UV light source. Apart from the absence of the pink anthocyanin spot, the C1-108 mutant's chromatogram did not show any differences in flavonoid pattern compared to C1-34 and C1-67 (Fig. 7B, right).

DISCUSSION

Indian mustard and *B. rapa* plants supplied with colorless molybdate accumulated a blue compound in the peripheral cell layers. This compound appears to be associated with Mo because the blue color intensity was correlated with Mo content of the seedlings (Fig. 2). Also, EDAX data showed accumulation of Mo in the epidermal layer (Fig. 3). XAS data indicated that Mo is accumulated in the form of polymolybdate(s) in the plant (Fig. 4). The blue color most likely arises from complexation of the polymolybdate(s) with anthocyanins (polymolybdates are colorless), for anthocyanin-less *B. rapa* mutants did not exhibit the blue coloration when supplied with molybdate (Fig. 5A). Furthermore, in anthocyanin-containing *B. rapa* varieties, the blue compound colocalized with the anthocyanins in the epidermal cell layer (Fig. 5B). Anthocyanin levels were positively related to Mo concentration in the three *B. rapa* varieties (Fig. 6). Our data were not conclusive with respect to a possible role of anthocyanins in Mo tolerance, for anthocyanin levels were positively correlated with Mo tolerance under some but not all experimental conditions tested.

The compound responsible for the observed effects appears to be anthocyanin, rather than some other flavonoid, for the following reasons. First, a purified anthocyanin extract showed an in vitro color change from pink to blue upon addition of molybdate (Fig. 7A). Second, based on fluorescence microscopy, the anthocyanin-less mutant appears to be able to produce flavonols (Fig. 7B), which are the last intermediates in the anthocyanin biosynthesis pathway before leucoanthocyanidins are formed (Dooner and Robbins, 1991). Also, paper chromatography showed that the anthocyanin-less seedlings contain all the UV-fluorescent products of the anthocyanin-containing varieties, but no anthocyanin (Fig. 7B).

Table III. *Mo tolerance of PPM-sterilized B. rapa varieties*

Seedlings were grown for 7 d on agar medium containing ammonium molybdate. Values shown represent relative growth, calculated as: (growth + Mo/growth − Mo) × 100% (mean ± SE, $n = 36$). *P* values represent a statistical comparison with the C1-108 line. C1-108, Anthocyaninless variety; C1-67, high anthocyanin variety. NS, Not significant ($P > 0.05$).

Variety	30 mg L^{-1} Mo		60 mg L^{-1} Mo	
	Fresh wt	Root length	Fresh wt	Root length
C1-108	60 ± 3	54 ± 3	33 ± 3	22 ± 2
C1-67	58 ± 2 (NS)	57 ± 3 (NS)	47 ± 2 ($P < 0.001$)	25 ± 2 (NS)

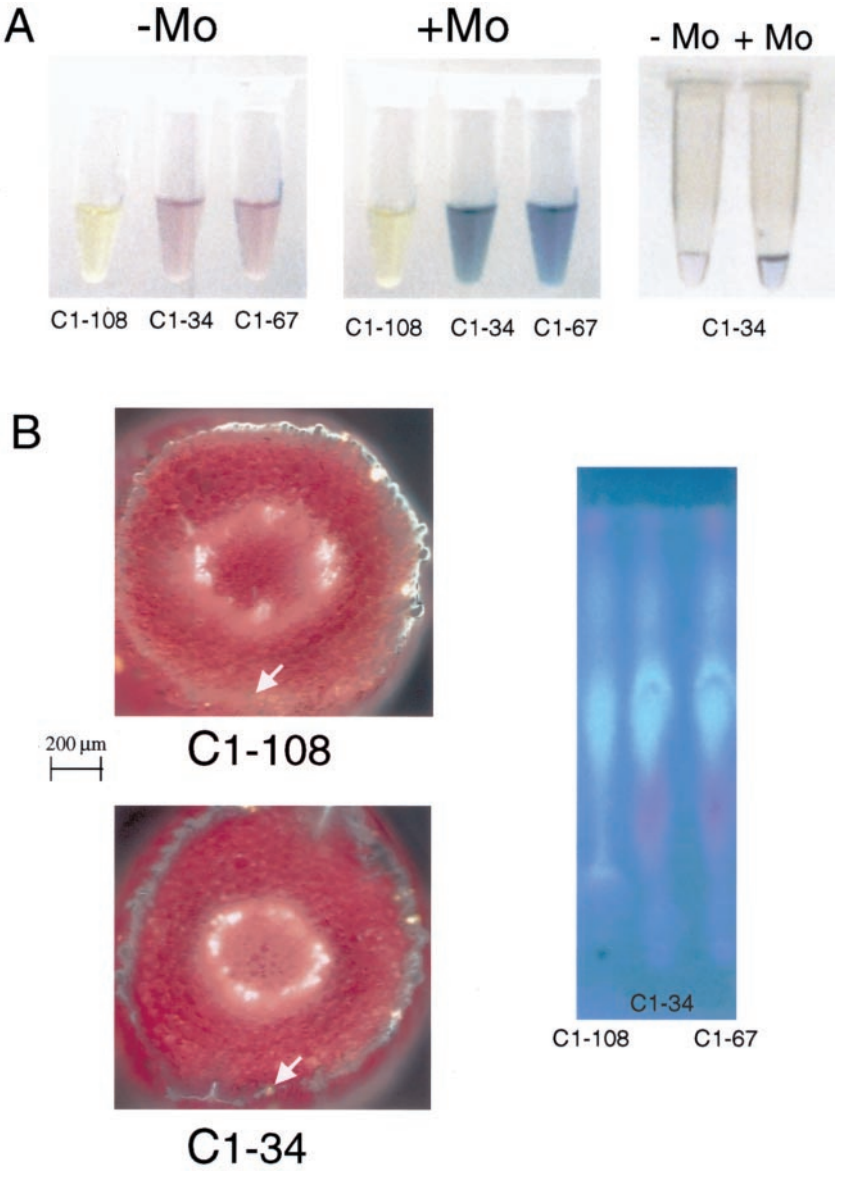

Figure 7. Anthocyanins appear to be involved in formation of a blue Mo compound. A, Anthocyanin extracts made from *B. rapa* C1-34 seedlings grown for 7 d on agar medium without Mo. Left, Extracts; middle, after in vitro addition of molybdate; right, after purification, before and after addition of molybdate. B, Detection of flavonols in the different *B. rapa* varieties grown for 7 d on agar medium without Mo. Left, Cross sections of hypocotyls, stained with diphenylboric acid-2-aminoethyl ester, visualized using a UV light source and 4,6-diamidino-2-phenylindole (DAPI) filter. The white arrows indicate the presence of flavonols, which stain orange. Note that other autofluorescence seen here is probably caused by sinapate esters (blue), chlorophyll (red), and xylem (white). Right, Paper chromatogram of flavonoid extracts, obtained using butanol:acetic acid:water (4:1:5, v/v) as the liquid phase.

Anthocyanins in the plant are mostly dissolved in cell fluids, but are sometimes present as crystals (Shibata et al., 1919). This is in accordance with what we have found because the blue compound exists as a water-soluble, crystalline precipitate.

This is the first time that anthocyanins have been proposed as having a function in metal accumulation or tolerance, although metal complexation has long been known to have a role in determining anthocyanin color (Elhabiri et al., 1997). Proposed roles for anthocyanins include attraction of pollinators and seed dispersers (Mol et al., 1996), UVB protection (Klaper et al., 1996), modification of the quality and quantity of captured light (Barker et al., 1997), defense from herbivory (Coley and Kusar, 1996), protection from photoinhibition (Dodd et al., 1998), and free radical scavenging (Yamasaki, 1997). It is known that anthocyanins are produced in response to stress (Chalker-Scott, 1999), and may be sequestered in response to ethylene (Zhou and Goldsbrough, 1993). Therefore, it is quite feasible that anthocyanins play a role in stress resistance.

The involvement of anthocyanins in Mo accumulation may be direct, through binding of the Mo, or indirect. Binding of Mo to anthocyanins may explain the color change to blue. Our XAS data indicate a change from four- to six-coordinate Mo, as well as longer range interactions. These observations, together with the vivid blue color of the plant material, initially suggested the possibility of in vivo formation of Mo blues or heteropoly blues. The former comprise a family of soluble molecules consisting of oxygen-coordinated polyhedra of Mo linked together to form giant wheel-shaped clusters (Müller and Serain, 2000), whereas the latter also involve MoO_n polyhedra, and additionally a heteroatom such as

four-coordinate phosphorus. However, the presence of these complexes is not consistent with the pH-dependent reversible color changes of the aqueous plant extracts observed in the present work (Müller and Serain, 2000). These observations are more consistent with the formation of a Mo-catecholate complex, such as a Mo-anthocyanin complex, in which there may be binding of one or more Mo of a polymolybdate anion at the ortho-dihydroxyl group on the B ring on the anthocyanin. A similar complexation of metals with anthocyanins has been reported for magnesium (Kondo et al., 1992), iron (Everest and Hall, 1921), and aluminum (Takeda et al., 1985). In each case, binding of these metals also resulted in a color change to blue. Therefore, it is likely that the anthocyanins directly bind the Mo, resulting in a blue product. In fact, molybdate is used in colorimetric assays of phenolics or lipids, in which the resulting product turns blue (Rouser et al., 1970). The involvement of anthocyanin is not expected to be obvious in the XAS data because both Mo-OH and Mo-O-(anthocyanin) would be expected to have very similar bond lengths, and only one Mo in the polymolybdate need be involved for effective complex formation.

The location of the Mo in the vacuoles of the epidermis (EDXA, 33 mM) corresponds with the intracellular location of anthocyanins (Alfenito et al., 1998). Other studies have also shown accumulation of metals in the vacuoles of the epidermis. For example, Heath et al. (1997) reported similar localization of nickel in the epidermis of *Thlaspi montanum* var *sikiyouense* leaves and Küpper et al. (1999) found zinc to compartmentalize in the epidermal vacuoles of the zinc hyperaccumulator, *Thlaspi caerulescens*. The observed correlation between dimension of cells and Mo content is also in agreement with results concerning Zn accumulation in *T. caerulescens* leaves, as reported by Küpper et al. (1999), who propose that vacuolation of epidermal cells may promote preferential Zn accumulation. Thus, sequestration of excess metals in the vacuoles of epidermal cells appears to be a common mechanism of metal accumulation and may play a role in tolerance. It is not clear what chelating agents are involved in accumulating various metals in the epidermal vacuoles. So far, compounds shown to be involved in the chelation of toxic metals are mostly peptides or organic acids (e.g. Steffens, 1990; Salt et al., 1995; Zenk, 1996; Larsen et al., 1998; Sagner et al., 1998; von Wiren et al., 1999). To our knowledge, this is the first time that a role for anthocyanin is proposed in metal sequestration.

The anthocyanin-containing *B. rapa* varieties accumulated more Mo in their shoots than anthocyanin-less plants because their Mo concentration was higher, and their biomass was equal or greater. It is feasible that anthocyanins facilitate vacuolar sequestration of Mo, thereby allowing plants to separate Mo from vital biochemical processes in other cell compartments. This separation reduces metal toxicity, resulting in better growth. Faster growth, in turn, is likely to enhance Mo accumulation because metal translocation through the xylem is thought to be driven by transpiration (Salt et al., 1995).

There are still many questions surrounding plant Mo uptake and metabolism. The requirement of plants for Mo is lower than that for any of the other mineral nutrients, except nickel (Marschner, 1995). Still, plants are fairly tolerant to Mo. Therefore, there must be some mechanism in plants whereby the toxic effects of Mo are reduced. This study suggests anthocyanin to be a part of that mechanism, and thereby sheds new light on both Mo metabolism and anthocyanin function in plants.

MATERIALS AND METHODS

Plant Material

Indian mustard (*Brassica juncea*) seeds (accession no. 173874) were obtained from the North Central Regional Plant Introduction Station (Ames, IA). *Brassica rapa* seeds (accession nos. C1-108, C1-34, and C1-67) were obtained from the Crucifer Genetics Cooperative Department of Plant Pathology (University of Wisconsin, Madison). The accession nos. correspond accordingly: C1-108 = anthocyanin-less variety, C1-34 = wild type, and C1-67 = high-anthocyanin variety.

Seedling Growth Experiments

Indian mustard seeds were sterilized by rinsing in 96% (v/v) ethanol for 30 s, then in 0.65% (w/v) hypochlorite solution for 30 min, and subsequently in sterile deionized water for 5 × 10 min, all on a rocking platform (Pilon-Smits et al., 1999).

B. rapa seeds were either sterilized using the procedure described above, or by soaking the seeds in 2% (w/v) PPM and incorporating 0.1% (w/v) PPM into the growth medium.

Fifty seeds were sown in a grid pattern in Magenta boxes (Sigma, St. Louis) on one-half-strength Murashige and Skoog medium with 10 g L^{-1} Suc and 4 g L^{-1} Agargel (Sigma), pH 5.8, with or without ammonium heptamolybdate tetrahydrate [$(NH_4)_6Mo_7O_{24}$] (Aldrich, Milwaukee, WI). Please note that one-half-strength Murashige and Skoog contains 0.125 mg L^{-1} Mo; therefore, the untreated controls were not Mo depleted. Indian mustard seedlings were supplied with 60 mg L^{-1} Mo and *B. rapa* seedlings were supplied with 30 or 60 mg L^{-1} Mo. Mo concentrations were chosen to give approximately 50% growth inhibition. For Indian mustard, this concentration was 60 mg L^{-1} Mo. *B. rapa* seedlings were more sensitive to Mo: 50% inhibition was reached at 30 mg L^{-1} Mo. Still, some experiments with *B. rapa* were carried out using 60 mg L^{-1} Mo to compare with Indian mustard. After 7 d at 25°C at 16-h-light and 8-h-dark photoperiod, individual seedlings were harvested, washed, and weighed, and the root length

was measured. Roots were removed and the shoots were dried overnight at 70°C for elemental analysis.

Mo Analysis

For the analysis of Mo content, dried plant samples (30 mg) were acid digested according to the method of Zarcinas et al. (1987). Mo concentrations were analyzed in the acid digests using inductively coupled plasma atomic emission spectrometry according to the method of Fassel (1978).

EDXA

Seeds of Indian mustard were germinated under sterile conditions as described above, on agar medium containing 130 mg L^{-1} Mo. This Mo concentration is higher than that used for other experiments with Indian mustard because EDXA requires high levels of Mo in the plant tissue for useful dotmaps to be collected. The seedlings were grown in a controlled environment under the following conditions: 16-h day length with a light intensity of 350 μmol photons m^{-2} s^{-1} supplied by fluorescent tubes, 20°C/16°C day/night temperature, and 60% to 70% relative humidity. After 10 d the seedlings were removed and x-ray microanalysis was performed on the stems ($n \geq 3$).

Sections of plant stems were excised and mounted in an Al vice. Samples were then rapidly (within less than 1 min after excision) frozen in liquid nitrogen and transferred to a fracturing chamber cooled to −170°C. A blade was used to cut through the cells. Samples subsequently were coated evaporatively with carbon. EDXA analysis was performed in a scanning electron microscope (XL 40, Philips, Eindhoven, The Netherlands) on a cryostage (−160°C to −180°C), using an acceleration voltage of 30 kV and a working distance of 10 mm. Spectra from 0 to 20 keV were collected at increments of 10 eV per channel with the electron beam focused on a rectangular area in the center of selected cells. The spectra were analyzed using the program Superquant (EDAX, San Francisco). A calibration between peak/background ratios for specific elements and their concentrations in the standard solutions was used to quantify the data recorded (Boekestein et al., 1984; Van Steveninck and Van Steveninck, 1991). The distribution of selected elements across a section of a sample was measured semiquantitatively by displaying the count rate within a narrow spectrum window within its peak (0.6× peak one-half width) along a line transect. A two-dimensional distribution pattern was also recorded by scanning an area of the specimen repeatedly for up to 2 h and integrating the counts for Mo, P, and K within their respective spectrum windows into dot maps.

XAS Analysis

Shoot and root tissues were collected from 7-d-old Indian mustard seedlings supplied with 60 mg L^{-1} Mo. The samples were frozen in liquid nitrogen, ground, and stored at −80°C. Comprehensive XAS of frozen plant tissues was carried out on beam line 4-3 of the SSRL, with a Si(220) double crystal monochromator, an upstream aperture of 1 mm, and no focusing optics. Samples, either ground plant material or dilute solutions of standards, were transferred to lucite cuvettes with mylar tape for windows. During data collection, the cuvettess were maintained at approximately 15 K in a flowing liquid helium cryostat. X-ray absorption spectra were measured in fluorescence using a 13-element germanium detector. Energy calibration was achieved by collecting the spectrum of elemental Mo in transmittance simultaneously with the data; the first energy inflection of the Mo K edge was assumed to be 20,003.9 eV.

XAS data were analyzed using the EXAFSPAK suite of programs (http://www-ssrl.slac.stanford.edu/exafspak). Extended EXAFS data were quantitatively fit (Pickering et al., 1999) using phase and amplitude functions generated using the program feff7 (Mustre de Leon et al., 1991; Rehr et al., 1991).

Plant Extractions and Flavonoid Analysis

To extract the blue compound, Indian mustard seedlings treated with 60 mg^{-1} L Mo were ground in liquid nitrogen using a mortar and pestle. Samples (0.5 g) were transferred to microcentrifuge tubes. One-milliliter aliquots of various solvents (methanol, chloroform, and water) were added to individual samples. The solutions were mixed, centrifuged to remove cell debris, and the supernatant was transferred to a new tube. We considered this solution to be a crude cell extract. The blue compound was most soluble in water; therefore, aqueous extracts were used for pH titration experiments. The pH of the solutions was changed gradually by adding dilute solutions of HCl or KOH, and color changes were monitored.

Anthocyanins and other flavonoids were extracted overnight at room temperature from fresh, untreated 7-d-old *B. rapa* seedlings in a 70% (v/v) methanol/1% (w/v) HCl solution. Plant material was removed via centrifugation, and the solutions were brought up to pH 5, using KOH, to mimic vacuolar conditions.

The resulting crude anthocyanin extracts of each *B. rapa* variety were spotted on chromatography paper (#1 Whatman Inc., Clifton, NJ). The chromatogram was developed in butanol:acetic acid:water (4:1:5, v/v), and viewed using a UV light source. Anthocyanins from C1-34 seedlings were isolated using the same procedure. The pink spot on the paper was cut out and placed in 1 mL of 70% (v/v) methanol/1% (w/v) HCL solution to allow the anthocyanins to elute. The purity of this anthocyanin isolate was confirmed by paper chromatography, using 1% (w/v) HCl as the liquid phase. To test the capacity of anthocyanins to form a blue product with Mo, ammonium molybdate crystals were added to the crude or pure anthocyanin extracts, and color changes were monitored visually.

Flavonol staining was done using 0.25% (w/v) DPBA and 0.02% (v/v) Triton X-100 solution (Murphy et al., 2000). The solution was mixed with gentle agitation for 48 h at room temperature (25°C) prior to use. Cross sections

of seedlings were stained with the DPBA solution immediately before visualization under a UV light source with a DAPI filter (excitation 340–380 nm, suppression 430 nm).

Statistical Analysis

Student's *t* tests were performed using the statistical software program JMP-IN from the SAS Institute (Cary, NC).

ACKNOWLEDGMENTS

We thank Lorrie Anderson for her help making the microscopic images. We also thank Jan Maas, Wendy Peer, and Angus Murphy for their helpful advice concerning flavonoid detection. We thank Mark de Souza, Adel Zayed, and Steve Whiting for their help with the XAS analyses, and the Crucifer Genetics Cooperative, Department of Plant Pathology (University of Wisconsin, Madison) for supplying seeds of the *B. rapa* varieties. We also thank Marinus Pilon and Dr. Edward I. Stiefel for helpful suggestions and for critically reading the manuscript.

Received January 22, 2001; returned for revision April 9, 2001; accepted April 30, 2001.

LITERATURE CITED

Alfenito MR, Souer E, Goodman CD, Buell R, Mol J, Koes R, Walbot V (1998) Functional complementation of anthocyanin sequestration in the vacuole by widely divergent glutathione S-transferase. Plant Cell **10:** 1135–1149

Barber SA (1995) Soil Nutrient Bioavailability: A Mechanistic Approach. John Wiley & Sons, Inc., New York

Barker DH, Seaton GGR, Robinson SA (1997) Internal and external photoprotection in developing leaves of the CAM plant *Cotyledon orbiculata*. Plant Cell Environ **20:** 617–624

Boekestein A, Thiel F, Stols ALH, Aouw E, Stadhouders AM (1984) Surface roughness and the use of a peak to background ration in the x-ray analysis of bio-organic bulk specimen. J Microsc **134:** 327–333

Chalker-Scott L (1999) Environmental significance of anthocyanins in plant stress response. Photochem Photobiol **70:** 1–9

Coley PD, Kusar TA (1996) Anti-herbivore defenses of young tropical leaves: physiological constraints and ecological tradeoffs. *In* SS Mulkey, RL Shazdon, AP Smith, eds, Tropical Forest Plant Ecophysiology. Chapman and Hall, New York, pp 305–335

Dodd IC, Critchley C, Woodall GS, Stewart GR (1998) Photoinhibition in differently colored juvenile leaves of *Syzgium* species. Exp Bot **49:** 1437–1445

Dooner HK, Robbins TP (1991) Genetic and developmental control of anthocyanin biosynthesis. Annu Rev Genet **25:** 173–199

Elhabiri M, Figueiredo P, Toki K, Saito N, Brouillard R (1997) Anthocyanin-aluminum and -gallium complexes in aqueous solution. J Chem Soc Perkin Trans **2:** 355–362

Everest AE, Hall AJ (1921) Anthocyanins and anthocyanidins: Part IV. Observations on (a) anthocyan colors in flowers and (b) the formation of anthocyans in plants. Proc R Soc B **92:** 150–162

Falciani F, Terao M, Goldwurm S, Ronchi A, Gatti A, Minoia C, Li Calzi M, Salmona M, Cazzaniga G, Garattini E (1994) Molybdenum (VI) salts convert the xanthene oxidoreductase apoprotein into the active enzyme in mouse L929 fibroblastic cells. Biochem J **298:** 69–77

Fassel VA (1978) Quantitative elemental analysis by plasma emission spectroscopy. Science **202:** 183–191

Gupta UC, Lipsett J (1981) Molybdenum in soils, plants and amimals. Adv Agron **34:** 73–115

Heath SM, SouthwortheD, D'Allura JA (1997) Localization of nickel in epidermal subsidiary cells of leaves of *Thlaspi montanum* var *sikiyouense* (Brassicaceae) using energy-dispersive X-ray microanalysis. Int J Plant Sci **158:** 184–188

Heuwinkel H, Kirkby EA, Bot JL, Marschner H (1992) Phosphorous deficiency enhances molybdenum uptake by tomato plants. Plant Nutr **15:** 549–568

Hille R (1996) The mononuclear molybdenum enzymes. Chem Rev **96:** 2757–2816

Kannan S, Ramani S (1978) Studies on molybdenum absorption and transport in bean and rice. Plant Physiol **62:** 179–181

Karmian N, Cox FR (1978) Adsorption and extractability of molybdenum in relation to some chemical properties of soils. Soil Sci Soc Am J **42:** 757–761

Klaper R, Frankel S, Barenbaum MR (1996) Anthocyanin content and UVB sensitivity in *Brassica rapa*. Photochem Photobiol **63:** 811–813

Kondo T, Yoshida K, Nakagawa A, Kawai T, Tamura H, Goto T (1992) Structural basis of blue-color development in flower petals from *Commelina communis*. Nature **358:** 515–518

Kuper J, Palmer T, Mendel R, Schwarz G (2000) Mutations in the molybdenum cofactor biosynthetic protein Cnx1G from *Arabidopsis thaliana* define functions for molybdopterin binding, molybdenum insertion, and molybdenum cofactor stabilization. Proc Natl Acad Sci USA **97:** 6475–6480

Küpper H, Zhao F, McGrath SP (1999) Cellular compartmentation of zinc in leaves of the hyperaccumulator *Thlaspi caerulescens*. Plant Physiol **119:** 305–311

Kutzler FW, Natoli CR, Misemer DK, Doniach S, Hodgson KO (1980) Use of one-electron theory for the interpretation of near edge structure in K-shell x-ray absorption spectra of transition metal complexes. J Chem Phys **73:** 3274–3288

Larsen PB, Degenhardt J, Tai C-Y, Stenzler LM, Howell SH, Kochian LV (1998) Aluminum-resistant *Arabidopsis* mutants that exhibit altered patterns of aluminum accumulation and organic acid release from roots. Plant Physiol **117:** 9–17

Marschner H (1995) Mineral Nutrition of Higher Plants. Academic Press, San Diego

Mol J, Jenkins G, Schäfer E, Weiss D (1996) Signal perception, transduction, and gene expression involved in anthocyanin biosynthesis. Crit Rev Plant Sci **15:** 525–557

Müller A, Serain C (2000) Soluble molybdenum blues: "des Pudels Kern." Accounts Chem Res **33:** 2–10

Murphy AS, Peer WA, Taiz L (2000) Regulation of auxin transport by aminopeptidases and endogenous flavonoids. Planta **211:** 315–324

Mustre de Leon J, Rehr JJ, Zabinsky SI, Albers RC (1991) Ab initio curved-wave x-ray-absorption fine structure. Phys Rev **B44:** 4146–4156

Palmgren MG, Harper JF (1999) Pumping with plant P-type ATPases. J Exp Bot **50:** 883–893

Pickering IJ, Prince RC, George GN, Rauser WE, Wickramasinghe WA, Watson AA, Dameron CT, Dance IG, Fairlie DP, Salt DE (1999) X-ray absorption spectroscopy of cadmium phytochelatin and model systems. Biochim Biophys Acta **1429:** 351–364

Pilon-Smits EAH, Hwang S, Lytle CM, Zhu Y, Tai JC, Bravo RC, Chen Y, Leustek T, Terry N (1999) Overexpression of ATP sulfurylase in Indian mustard leads to increased selenate uptake, reduction, and tolerance. Plant Physiol **119:** 123–132

Rehr JJ, Mustre de Leon J, Zabinsky SI, Albers RC (1991) Theoretical x-ray absorption fine structure standards. J Am Chem Soc **113:** 5135–5140

Rouser G, Fleisher S, Yamamoto A (1970) Two-dimensional thin layer chromatographic separation of polar lipids and determination of phospholipids by phosphorous analysis of spots. Lipids **5:** 494–496

Sagner S, Kneer R, Wanner G, Cosson J-P, Deus-Neumann B, Zenk MH (1998) Hyperaccumulation, complexation and distribution of nickel in *Sebertia acuminata*. Phytochemistry **47:** 339–347

Salt DE, Price RC, Pickering IJ, Raskin I (1995) Mechanisms of cadmium mobility and accumulation in Indian mustard. Plant Physiol **109:** 1427–1433

Seo M, Akaba S, Oritani T, Delarue M, Bellini C, Caboche M, Koshiba T (1998) Higher activity of an aldehyde oxidase in the auxin-overproducing *superroot1* mutant of *Arabidopsis thaliana*. Plant Physiol **116:** 687–693

Shibata K, Shibata Y, Kasiwagi I (1919) Studies on anthocyanins: color variation in anthocyanins. J Am Chem Soc **41:** 208–220

Stallmeyer B, Schwarz G, Schulze J, Nerlich A, Kirsh J, Mendel RR (1999) The neurotransmitter receptor-anchoring protein gephyrin reconstitutes molybdenum cofactor biosynthesis in bacteria, plants and mammalian cells. Proc Natl Acad Sci USA **96:** 1333–1338

Stark JM, Redente EF (1990) Copper fertilization to prevent molybdenosis on retorted oil shale disposal piles. J Environ Qual **19:** 50–504

Steffens JC (1990) The heavy metal-binding peptides of plants. Annu Rev Plant Physiol Mol Biol **41:** 553–575

Stout PR, Meagher WR, Pearson GA, Johnson CM (1951) Molybdenum nutrition of plant crops: I. The influence of phosphate and sulfate on the absorption of molybdenum from soils and solution cultures. Plant Soil **3:** 51–87

Takeda K, Kariuda M, Itoi H (1985) Blueing of sepal color of *Hydrangea macrophylla*. Phytochemistry **24:** 2251–2254

Trlica MJ, Brown LF (2000) Reclamation of URAD molybdenum tailing: 20 years of monitoring change. *In* W Keammerer, ed, Proceedings of the High Altitude Revegetation Workshop, No. 14, Fort Collins, CO. Cooperative Extension Resource Center, Colorado State University, Fort Collins, CO, pp 82–133

Van Steveninck RFM, Van Steveninck ME (1991) Microanalysis. *In* JL Hall, C Hawes, eds, Electron Microscopy of Plant Cells. Acad Press, London, pp 415–455

von Wiren N, Sukhbinder K, Bansal S, Briat J-F, Khodr H, Shiori T, Leigh RA, Hider RC (1999) Nicotianamine chelates both FeIII and FeII: implications for metal transport in plants. Plant Physiol **119:** 1107–1114

Yamasaki H (1997) A function of color. Trends Plant Sci **2:** 7–8

Zarcinas BA, Cartwright B, Spouncer LR (1987) Nitric acid digestion and multi-element analysis of plant material by inductively coupled plasma spectrometry. Comm Soil Sci Plant Anal **18:** 131–146

Zenk MH (1996) Heavy metal detoxification in higher plants: a review. Gene **179:** 21–30

Zhou J, Goldsbrough PB (1993) An *Arabidopsis* gene with homology to glutathione S-transferase is regulated by ethylene. Plant Mol Biol **22:** 517–523